Mechanics of Materials 158 (2021) 103845

Contents lists available at ScienceDirect

Mechanics of Materials

journal homepage: www.elsevier.com/locate/mechmat

Lap shear of a soft and elastic adhesive

Yecheng Wang [a], Guodong Nian [a], Xuxu Yang [b], Zhigang Suo [a,*]

[a] John A. Paulson School of Engineering and Applied Sciences, Kavli Institute for Bionano Science and Technology, Harvard University, Cambridge, MA 02138, United States

[b] Department of Engineering Mechanics, Zhejiang University, Hangzhou 310027, China

ARTICLE INFO

Keywords:
Lap shear
Shear lag
Energy release rate
Soft and elastic adhesive
Elastic adherend

ABSTRACT

This paper studies the lap shear, in which both the adhesive and adherends are elastic, but the adhesive is much softer than the adherends. The shear lag model identifies a length, called the shear lag length L_s. The energy release rate of a debond crack is affected by the elasticity of both the adhesive and adherends. Their relative importance is characterized by the ratio of the length of the remaining joint, L, to the shear lag length, L_s. In the short-joint limit, $L/L_s \to 0$, the adherends do not deform, and the elasticity of the adhesive gives the energy release rate. In the long-joint limit, $L/L_s \to \infty$, the interior of the adhesive does not deform, and the elasticity of the adherends gives the energy release rate. The shear lag model gives an approximate expression of the energy release rate for all values of L/L_s. This expression is in excellent agreement with the results obtained by finite element calculations, so long as the crack is long compared to the thickness of the adhesive.

1. Introduction

When two thick books are interleaved page by page, pulling them apart is difficult. Watch this YouTube video (https://youtu.be/AX_lCOjLCTo). This phenomenon, called *shear lag*, is understood as follows. The interleaved books resist the pull by friction between the pages. The force needed to pull the books apart scales with the area of each page and the number of pages. Shear lag enables tough composites (Cottrell, 1964) and jamming structures (Narang et al., 2020), and is commonly analyzed using the *shear lag model* (Cox, 1952; Hui et al., 2018; Marshall and Cox, 1987). Shear lag also enables the *lap shear joint*, in which two adherends are joined over a large area by a thin layer of an adhesive (Jeevi et al., 2019). Even when the adhesive is weak, a lap shear joint can resist a large applied force. Lap shear joint can also be a nuisance, e.g., in deicing (Golovin et al., 2019). A lap shear joint is commonly evaluated by the *lap shear test*, where forces are applied to shear the two adherends apart. The lap shear test simulates a common mode of failure of an adhesive joint.

Lap shear test has been used to measure adhesion strength (Ni et al., 2020; Roy et al., 2015; Vakalopoulos et al., 2015; Yuk et al., 2019) and adhesion toughness (Hutchinson and Suo, 1991; Kendall, 1975a, b). The distinction of the two types of measurements is commonly misunderstood, as noted in recent papers (Golovin et al., 2019; Wang et al., 2020). Here we focus on a lap shear joint in which both the adhesive and the adherends are elastic. The energy release rate of a debond crack is often analyzed by neglecting the elasticity of the adhesive (Golovin et al., 2019; Kendall, 1975a, b). We have recently shown that such an analysis is inapplicable when the adhesive is extremely soft compared to the adherends (Wang et al., 2020). For example, in a joint of a hydrogel adhesive between two plastic tapes, the ratio of the elastic moduli of the adherends and adhesive is on the order of 10^6. In such a case, the adherends may deform negligibly and behave like rigid bodies, and the energy release rate comes entirely from the elasticity of the adhesive. The transition between the two types of behavior depends on the moduli of the adhesive and adherends, their thicknesses, as well as the length of the joint. Our previous paper identified the two limits, but did not present a model to analyze the transition.

This transition is the focus of the present paper. The shear lag model is used to derive the stress distributions in a lap shear joint without crack (Section 2). We assume linear elasticity in the adherends, but allow large shear deformation in the adhesive. The model identifies the *shear lag length*, L_s. The behavior of the joint is characterized by the ratio of the length of the joint, L, to the shear lag length, L_s. In the short-joint limit, $L/L_s \to 0$, the adherends do not deform and behave like rigid bodies, and the shear stress in the adhesive is nearly uniform. In the long-joint limit, $L/L_s \to \infty$, the adherends deform elastically, and the shear stress concentrates near each edge of the joint within a length scaled by L_s and vanishes in the interior of the adhesive. The shear lag model is also used

* Corresponding author.
E-mail address: suo@seas.harvard.edu (Z. Suo).

https://doi.org/10.1016/j.mechmat.2021.103845
Received 23 November 2020; Received in revised form 28 January 2021; Accepted 19 March 2021
Available online 26 March 2021

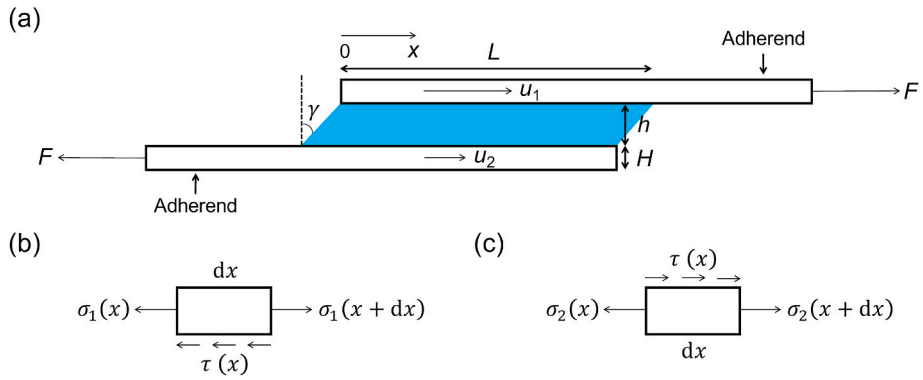

Fig. 1. Shear lag model. (a) An adhesive is sandwiched between two adherends. The origin of the coordinate x coincides with the left edge of the joint. When the adherends are pulled, tensile stresses $\sigma_1(x)$ and $\sigma_2(x)$ develop in the two adherends, and shear stress $\tau(x)$ develops in the adhesive. (b) Free-body diagram of an infinitesimal segment of the top adherend. (c) Free-body diagram of an infinitesimal segment of the bottom adherend.

to derive an approximate expression of the energy release rate of a debond crack for all values of L/L_s (Section 3). The energy release rate comes from the elasticity of the adhesive in the short-joint limit, and from the elasticity of the adherends in the long-joint limit. The approximate expression is in excellent agreement with the finite element calculations, so long as the crack is long compared to the thickness of the adhesive (Section 4).

2. Distribution of stresses in a lap shear joint without crack

An adhesive, width w and thickness h, is sandwiched between two adherends, thickness H (Fig. 1a). The thicknesses of the adhesive and adherends are taken to be small compared to the length of the joint, L. Let the origin of the coordinate x coincide with the left edge of the adhesive. The adherends are pulled by the force F. The shear lag model is usually developed for the setup in which only one adherend undergoes tensile deformation, but the approach is readily generalized for the setup here, where the two adherends undergo tensile deformation. Following the common practice in formulating a shear lag model, we assume that the stress state is shear in the adhesive, and is tension in the adherends.

Each adherend is modeled as a linear elastic material. In the top adherend, the tensile stress is linear in the tensile strain:

$$\sigma_1(x) = E\frac{\mathrm{d}u_1(x)}{\mathrm{d}x} \tag{1}$$

where $\sigma_1(x)$ and $u_1(x)$ are the tensile stress and displacement in the top adherend, and E is Young's modulus. A similar equation holds in the bottom adherend:

$$\sigma_2(x) = E\frac{\mathrm{d}u_2(x)}{\mathrm{d}x} \tag{2}$$

The adhesive can undergo large shear deformation:

$$\tan\gamma = \frac{u_1(x) - u_2(x)}{h} \tag{3}$$

The shear strain varies in the adhesive, $\gamma(x)$. The shear lag model assumes this shear strain to be the only mode of deformation in the adhesive. That is, the deformation gradient in the adhesive is approximated as

$$\mathbf{F} = \begin{bmatrix} 1 & \tan\gamma & 0 \\ 0 & 1 & 0 \\ 0 & 0 & 1 \end{bmatrix} \tag{4}$$

We model the adhesive as a neo-Hookean material (Ogden, 1997). The true stress σ_{ij} relates to the deformation gradient F_{iK} by $\sigma_{ij} = \mu F_{iK}F_{jK} - \Pi\delta_{ij}$, where μ is the shear modulus, and Π is the Lagrange multiplier that enforces incompressibility $\det\mathbf{F} = 1$. Consequently, the shear stress in the adhesive, $\tau = \sigma_{12}$, relates to the displacements as

$$\tau(x) = \mu\tan\gamma = \mu\frac{u_1(x) - u_2(x)}{h} \tag{5}$$

All other components of stress in the adhesive are taken to vanish. In the shear lag model, the finite deformation of a neo-Hookean adhesive relates the shear stress in the adhesive linearly to the difference in the displacements in the adherends.

The balance of forces in the top adherend requires that (Fig. 1b)

$$\frac{\mathrm{d}\sigma_1(x)}{\mathrm{d}x} = \frac{\tau(x)}{H} \tag{6}$$

Similarly, the balance of forces in the bottom adherend requires that (Fig. 1c)

$$\frac{\mathrm{d}\sigma_2(x)}{\mathrm{d}x} = -\frac{\tau(x)}{H} \tag{7}$$

A combination of the above equations leads to a second-order ordinary differential equation:

$$\frac{\mathrm{d}^2[u_1(x) - u_2(x)]}{\mathrm{d}x^2} = 2\frac{u_1(x) - u_2(x)}{L_s^2} \tag{8}$$

The equation identifies the shear lag length:

$$L_s = \sqrt{\frac{EhH}{\mu}} \tag{9}$$

When the adhesive is much softer than the adherends, the shear lag length can be much larger than the thicknesses of the adhesive and adherends. Taking representative values $E \sim 1$ GPa, $h \sim 1$ mm, $H \sim 10\ \mu$m, and $\mu \sim 1$ kPa, we estimate the shear lag length as $L_s \sim 10$ cm. The ratio $E/\mu \sim 10^6$ is representative of a hydrogel sandwiched between plastic tapes used in our previous experiments (Wang et al., 2020). This enormous ratio of moduli can be compared with that in a common lap shear joint, where epoxy adheres two metals, $E/\mu \sim 100$ GPa/1 GPa $\sim 10^2$.

A general solution to equation (8) is

$$u_1(x) - u_2(x) = A\exp\left(\frac{\sqrt{2}x}{L_s}\right) + B\exp\left(-\frac{\sqrt{2}x}{L_s}\right) \tag{10}$$

where A and B are constants to be determined by boundary conditions. The shear stress in the adhesive is

$$\tau(x) = \frac{\mu}{h}\left[A\exp\left(\frac{\sqrt{2}x}{L_s}\right) + B\exp\left(-\frac{\sqrt{2}x}{L_s}\right)\right] \tag{11}$$

An integration of (6) gives the tensile stress in the top adherend:

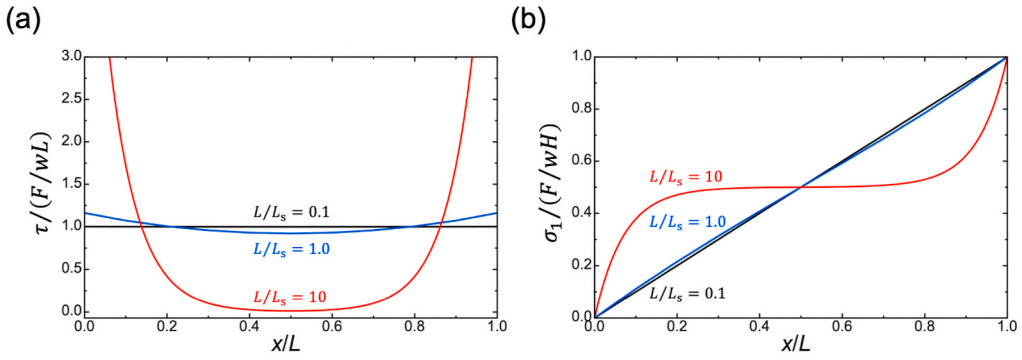

Fig. 2. Stress distribution along the direction of length for several values of the normalized joint length. (a) Shear stress distribution in the adhesive. (b) Tensile stress distribution in the top adherend.

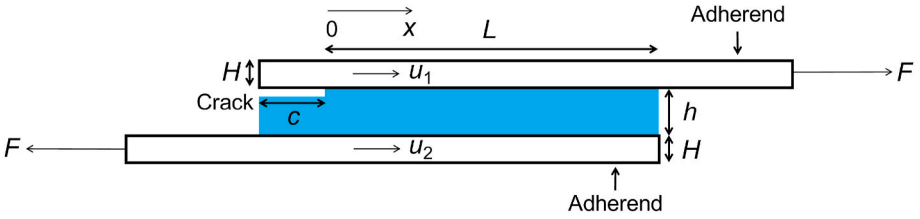

Fig. 3. A crack, length c, is precut either in the adhesive or on the interface between the adhesive and one adherend.

$$\sigma_1(x)=\frac{L_s\mu}{\sqrt{2}hH}\left\{A\left[\exp\left(\frac{\sqrt{2}x}{L_s}\right)-1\right]-B\left[\exp\left(-\frac{\sqrt{2}x}{L_s}\right)-1\right]\right\} \tag{12}$$

In obtaining this equation, we have used a boundary condition $\sigma_1(0)=0$. Note that $\sigma_1(L)=F/wH$ and by symmetry $\sigma_1(L/2)=F/2wH$. These two conditions give that

$$A=\frac{\frac{L_sF}{\sqrt{2}EwH}\left[1+\exp\left(-\frac{\sqrt{2}L}{L_s}\right)\right]}{\exp\left(\frac{\sqrt{2}L}{L_s}\right)-\exp\left(-\frac{\sqrt{2}L}{L_s}\right)} \tag{13}$$

and

$$B=\frac{\frac{L_sF}{\sqrt{2}EwH}\left[1+\exp\left(\frac{\sqrt{2}L}{L_s}\right)\right]}{\exp\left(\frac{\sqrt{2}L}{L_s}\right)-\exp\left(-\frac{\sqrt{2}L}{L_s}\right)} \tag{14}$$

The stress in the bottom adherend is given by $\sigma_2(x)=\frac{F}{wH}-\sigma_1(x)$.

The shear stress in the adhesive, $\tau(x)$, normalized by the average shear stress, F/wL, is plotted for several values of the normalized joint length, L/L_s (Fig. 2a). When the joint is short, $L/L_s\to 0$, the shear stress in the adhesive is nearly uniform, well approximated by $\tau=F/wL$. When the joint is long, $L/L_s\to\infty$, the shear stress in the adhesive concentrates near the edges of the adhesive over a length scaled by L_s, and vanishes in the interior of the adhesive.

The tensile stress in the top adherend, $\sigma_1(x)$, normalized by the applied tensile stress, F/wH, is plotted for several values of the normalized joint length, L/L_s (Fig. 2b). When the joint is short, $L/L_s\to 0$, the shear stress in the adhesive is nearly uniform, and the tensile stress in the adherend is linear in x. In this limit, the two adherends act like rigid bodies. When the joint is long, $L/L_s\to\infty$, the shear stress in the adhesive concentrates near the edges and vanishes in the interior, and the tensile stress in the adherend varies steeply near the edges and becomes uniform in the interior. In this limit, the two adherends deform appreciably. In the top adherend, the tensile stress vanishes at the left edge, plateaus at the half of the applied stress, $F/2wH$, and then rises to the applied stress, F/wH, at the right edge. The effects of edges are confined within a length scaled by L_s. In the interior, when the tensile stress plateaus, the two adherends carry the tensile stress equally.

3. Energy release rate of a debond crack

We calculate the energy release rate for a crack, length c, precut either in the adhesive or on the interface between the adhesive and one adherend (Fig. 3). Let the origin of the coordinate x coincide with the crack front, which is also the left edge of the remaining joint. Let L be the length of the remaining joint. We have previously identified two limiting cases (Wang et al., 2020). In the short-joint limit, $L/L_s\to 0$, the adherends behave like rigid bodies, and the energy release rate is governed by the elasticity of the adhesive, given by $hW(\gamma)$, where $W(\gamma)$ is the elastic energy of the deformed adhesive per unit volume (Wang et al., 2020). When the adhesive obeys the neo-Hookean model, the energy density is $W=\mu(F_{iK}F_{iK}-3)/2$, and the energy release rate is

$$G=\frac{h}{2\mu}\left(\frac{F}{wL}\right)^2 \tag{15}$$

In the long-joint limit, $L/L_s\to\infty$, the interior of the adhesive does not carry stress and the adherends deform. In the debonded part, only one adherend far behind the crack front carries stress, F/wH, and the elastic energy of the adherend per unit length is $\frac{H}{2E}\left(\frac{F}{wH}\right)^2$. In the bonded part, both adherends far ahead the crack front carry stress, the stress in each adherend is $F/2wH$ (Fig. 2b), and the elastic energy of the two adherends per unit length is $\frac{H}{4E}\left(\frac{F}{wH}\right)^2$. The energy release rate is determined by the difference in the elastic energy per unit length of the two parts (Kendall, 1975a):

$$G=\frac{H}{4E}\left(\frac{F}{wH}\right)^2 \tag{16}$$

We now derive a general expression of the energy release rate. The elastic energy of the system is

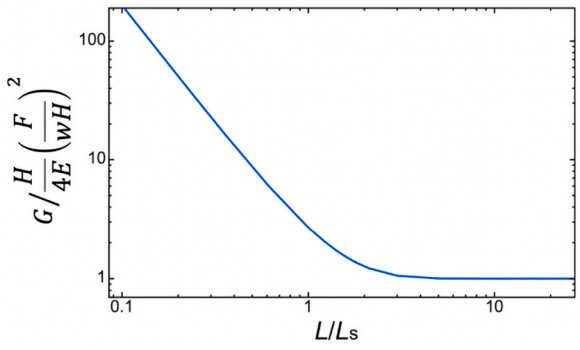

Fig. 4. Normalized energy release rate as a function of the normalized length of the remaining joint.

$$U=\frac{hw}{2\mu}\int_0^L \tau^2(x)\mathrm{d}x+\frac{Hw}{2E}\int_0^L \sigma_1^2(x)\mathrm{d}x+\frac{Hw}{2E}\int_0^L \sigma_2^2(x)\mathrm{d}x+\frac{Hwc}{2E}\left(\frac{F}{wH}\right)^2 \tag{17}$$

The first term is the elastic energy of the adhesive, the second term is the elastic energy of the top adherend, the third term is the elastic energy of the bottom adherend, and the last term is the elastic energy of the debonded part of the adherend.

Under prescribed load, the energy release rate is defined by

$$G=\frac{\partial U(\sigma,c)}{w\partial c} \tag{18}$$

When the debond crack extends by dc, the remaining joint shortens by the same amount, dL = − dc. The energy release rate is

$$G=\frac{H}{4E}\left(\frac{F}{wH}\right)^2\left[\frac{\exp\left(\frac{\sqrt{2}L}{L_s}\right)+1}{\exp\left(\frac{\sqrt{2}L}{L_s}\right)-1}\right]^2 \tag{19}$$

An inspection of the geometry in Fig. 3 indicates that, within the approximation of the shear lag model, the energy release rate G should be a function of the length of the remaining joint, L. This expression approaches the two limits (15) and (16). The energy release rate (19) is plotted in a dimensionless form (Fig. 4). In the short-joint limit, $L/L_s\to 0$, the adherends do not deform, and the elasticity of the adhesive gives the energy release rate, $G=\frac{h}{2\mu}\left(\frac{F}{wL}\right)^2$. In the long-joint limit, $L/L_s\to\infty$, the interior of the adhesive does not deform, and the elasticity of the adherends gives the energy release rate, $G=\frac{H}{4E}\left(\frac{F}{wH}\right)^2$. When the length of the debond crack increases, the length of the remaining joint decreases. When the remaining joint is short, the energy release rate increases as the crack extends, indicating unstable crack growth. When the remaining joint is long, the energy release rate is constant as the crack extends, indicating stable crack growth if the load machine is displacement-controlled.

4. Finite element analysis

The shear lag model only approximately describes the stress field in the lap shear joint. To ascertain the predictions of the shear lag model, we calculate distribution of the shear stress in the adhesive and the energy release rate using the finite element software ABAQUS.

We apply a prescribed displacement to the left end of the top adherend and fix the right end of the bottom adherend. 4-node bilinear plane strain quadrilateral elements (CPE4R) are used for both the adhesive and adherends. The adhesive and the adherends are taken to obey the neo-Hookean model and the linear elastic model, respectively. To calculate the energy release rate, contour integrals are adopted and a ring of collapsed quadrilateral elements are used to model the singularity at the crack tip. The mesh close to the crack tip is refined to ensure accuracy. We set E = 920 MPa, H = 50 μm, μ = 2.634 kPa, and h = 4.5 mm. These values are representative of those in our previous experiments (Wang et al., 2020). Corresponding to these values, the shear lag length is L_s = 28 cm.

We compare the analytical result and the finite element calculation of the normalized shear stress of the top layer of the adhesive for various normalized joint lengths, L/L_s (Fig. 5). This comparison corroborates the significance of the shear lag length. When $L/L_s\to 0$, the shear stress is uniformly distributed in the adhesive and is well approximated by $\tau = F/wL$. When $L/L_s\to\infty$, the shear stress concentrates near the edges and vanishes in the interior of the adhesive, so that $\tau \ll F/wL$. The finite element calculations give the stress concentrations and singularities near the edges, which cannot be captured by the shear lag model.

To appreciate the applicability of the analytical results obtained in this work, we plot the analytical expression of the normalized energy release rate, $G/\frac{H}{4E}\left(\frac{F}{wH}\right)^2$, as a function of the normalized joint length,

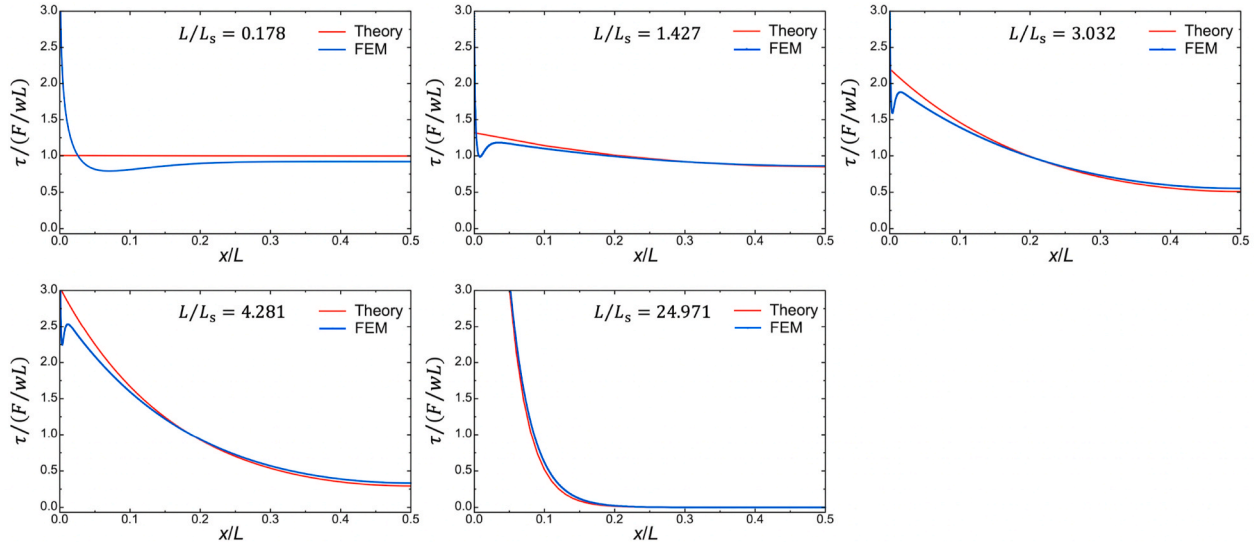

Fig. 5. Comparison between theory and finite element calculation of the normalized shear stress distribution of the top layer of the adhesive along the direction of length for various normalized joint lengths. The theoretical prediction and the finite element calculations are consistent with each other.

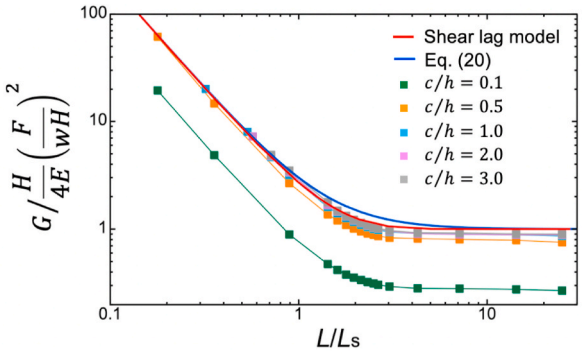

Fig. 6. Comparison between theory and finite element calculation of the normalized energy release rate as a function of the normalized joint length for various normalized crack lengths. The analytical expression (19) and the finite element calculations are consistent with each other when the crack is long compared to the thickness of the adhesive.

L/L_s, and compare it with the finite element calculations for various normalized crack lengths, c/h (Fig. 6). So long as the crack length is large compared to the adhesive thickness, the expression of the shear lag model (19) agrees well with the finite element calculations for all values of L/L_s.

Also plotted is the approximate expression of the energy release rate (Wang et al., 2020):

$$G = \frac{h}{2\mu}\left(\frac{F}{wL}\right)^2 + \frac{H}{4E}\left(\frac{F}{wH}\right)^2 \tag{20}$$

The approximate solution (20) is exact in the two limits, but differs from the prediction of the shear lag model (19) for a joint of intermediate length.

5. Conclusion

We have studied the lap shear of a soft and elastic adhesive. When the adhesive is extremely soft compared to the adherends, the shear lag length is much larger than the thickness of the joint. We have used the shear lag model to derive an analytical expression for the energy release rate for a debond crack. The energy release rate comes from the elasticity of the adhesive in the short-joint limit, and from the elasticity of the adherends in the long-joint limit. The analytical expression agrees well with the finite element calculations when the length of the crack is large compared to the thickness of the adhesive.

Declaration of competing interest

The authors declare no competing interest.

Acknowledgement

This research was supported by NSF through the Harvard University Materials Research Science and Engineering Center DMR-2011754.

References

Cottrell, A.H., 1964. Strong solids. Proc. R. Soc. A 282, 2–9.
Cox, H.L., 1952. The elasticity and strength of paper and other fibrous materials. Br. J. Appl. Phys. 3, 72–79.
Golovin, K., Dhyani, A., Thouless, M.D., Tuteja, A., 2019. Low-interfacial toughness materials for effective large-scale deicing. Science 364, 371–375.
Hui, C.-Y., Liu, Z., Minsky, H., Creton, C., Ciccotti, M., 2018. Mechanics of an adhesive tape in a zero degree peel test: effect of large deformation and material nonlinearity. Soft Matter 14, 9681–9692.
Hutchinson, J.W., Suo, Z., 1991. In: Hutchinson, J.W., Wu, T.Y. (Eds.), Mixed Mode Cracking in Layered Materials. Adv. Appl. Mech. Elsevier, pp. 63–191.
Jeevi, G., Nayak, S.K., Abdul Kader, M., 2019. Review on adhesive joints and their application in hybrid composite structures. J. Adhes. Sci. Technol. 33, 1497–1520.
Kendall, K., 1975a. Crack propagation in lap shear joints. J. Phys. D Appl. Phys. 8, 512–522.
Kendall, K., 1975b. Cracking of short lap joints. J. Adhes. 7, 137–140.
Marshall, D.B., Cox, B.N., 1987. Tensile fracture of brittle matrix composites: influence of fiber strength. Acta Metall. 35, 2607–2619.
Narang, Y.S., Aktaş, B., Ornellas, S., Vlassak, J.J., Howe, R.D., 2020. Lightweight highly tunable jamming-based composites. Soft Robot. 7, 724–735.
Ni, X., Chen, C., Li, J., 2020. Interfacial fatigue fracture of tissue adhesive hydrogels. Extreme. Mech. Lett. 34, 100601.
Ogden, R.W., 1997. Non-linear Elastic Deformations. Courier Corporation.
Roy, C.K., Guo, H.L., Sun, T.L., Ihsan, A.B., Kurokawa, T., Takahata, M., Nonoyama, T., Nakajima, T., Gong, J.P., 2015. Self-adjustable adhesion of polyampholyte hydrogels. Adv. Mater. 27, 7344–7348.
Vakalopoulos, K.A., Wu, Z., Kroese, L., Kleinrensink, G.-J., Jeekel, J., Vendamme, R., Dodou, D., Lange, J.F., 2015. Mechanical strength and rheological properties of tissue adhesives with regard to colorectal anastomosis: an ex vivo study. Ann. Surg. 261, 323–331.
Wang, Y., Yang, X., Nian, G., Suo, Z., 2020. Strength and toughness of adhesion of soft materials measured in lap shear. J. Mech. Phys. Solids. 143, 103988.
Yuk, H., Varela, C.E., Nabzdyk, C.S., Mao, X., Padera, R.F., Roche, E.T., Zhao, X., 2019. Dry double-sided tape for adhesion of wet tissues and devices. Nature 575, 169–174.